Soil Moisture Active Passive (SMAP) Observer Power System Architecture

Harry Aintablian, Christopher Stell, Gregory Carr
Jet Propulsion Laboratory, California Institute of Technology.

Abstract

The Soil Moisture Active and Passive (SMAP) observer is scheduled for launch in 2014. The primary science objective of SMAP is the high-resolution mapping of earth's soil moisture. These measurements will be used to enhance understanding of processes that link the water, energy and carbon cycles, and to extend the capabilities of weather and climate prediction models. The SMAP orbit, sun-synchronous with an altitude of 680 km, was chosen to optimize the sampling characteristics of the instruments while ensuring that the resolution requirements are met. The combined active radar and passive radiometer measurement approach takes advantage of the spatial resolutions of the radar (3 km x 1000 km) and the radiometer (39 km x 47 km).

The SMAP observer is powered by a multi-panel deployable, fixed configuration solar array. Li-Ion batteries provide power during launch, eclipse and safe periods of the mission. The 28V power bus voltage is controlled by solar array segment switching. This paper describes the SMAP power system architecture. In addition, it details the power system's unique approach to controlling the power bus and charging the battery. It presents simulation results that validate the bus control concept.

1 Mission Overview

The primary science objective of the SMAP mission is to provide high-resolution mapping of earth's surface moisture and its freeze/thaw state. SMAP measurements will enable scientists to:

- Estimate global water and energy fluxes at the surface of the earth
- Enhance weather and climate forecast skills
- Develop improved flood and drought predictions
- Understand processes that link terrestrial water, energy, and carbon cycles
- Quantify carbon fluxes in boreal landscapes

The SMAP instruments incorporate a radar and a radiometer sharing a single L-band feed and a spinning deployable mesh antenna. The 6-m diameter antenna rotates about the nadir axis at 14.6 rpm, producing conically scanned antenna beam with a surface incidence angle of approximately 40 degrees (Figure 1).

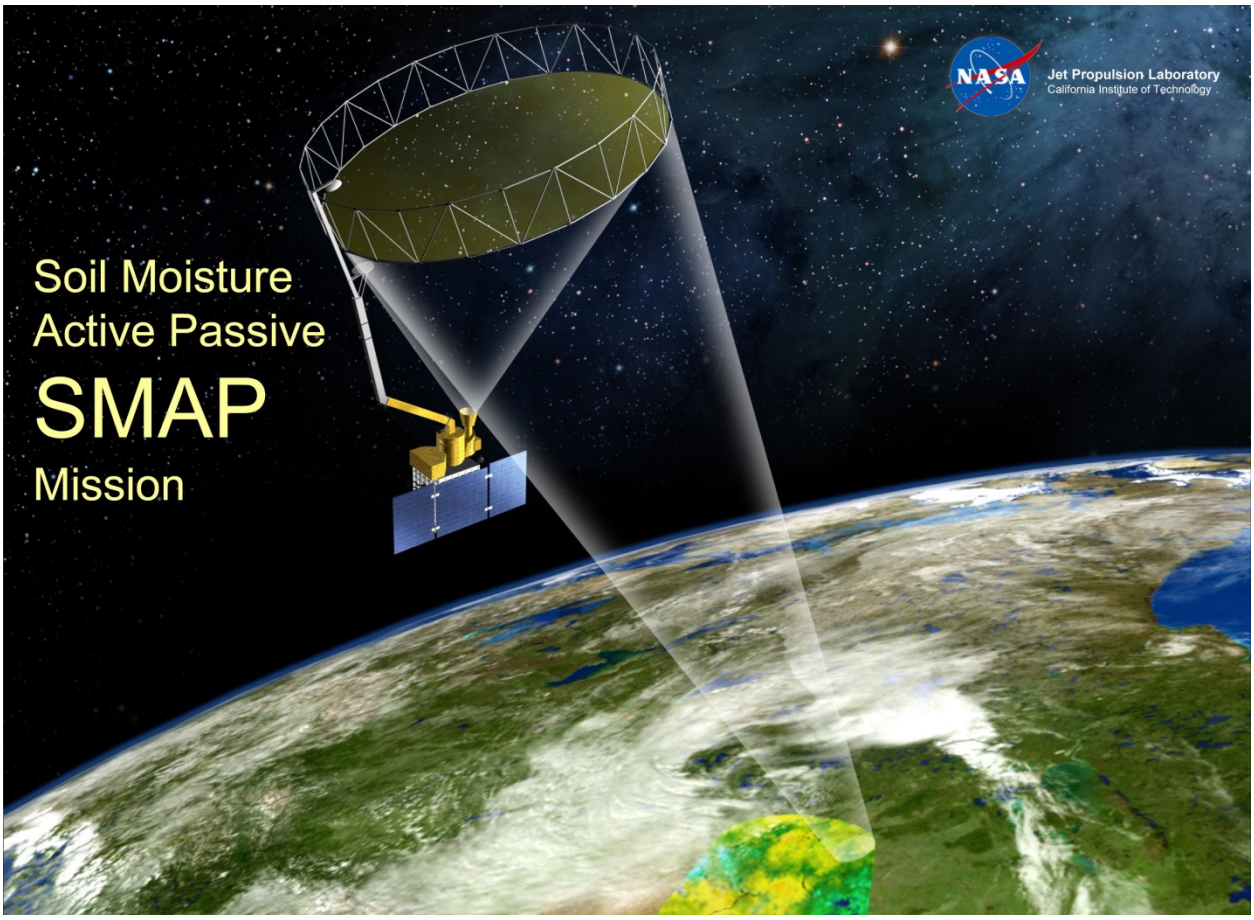

Figure 1: SMAP Observer

The radiometer has a spatial resolution of 40 km, while the radar yields a spatial resolution of 1 – 3 km. By combining the attributes of the radar and radiometer observations, soil moisture data is retrieved at a spatial resolution of 10 km, and a freeze-thaw state at a spatial resolution of 3 km. SMAP science measurements will be acquired for a period of three years in order to capture positive and negative seasonal anomalies in the water, energy, and carbon cycles across environmentally diverse regions of the globe.

2 Description of SMAP Power System Architecture

The SMAP power system architecture is derived from a fault tolerant architecture typically used on many JPL missions. This architecture employs modularity, scalability and standardized interfaces and the designs are expandable to meet various mission power needs. The architecture separates the power bus control function from the power distribution function to enable the ability to adapt to different mission specific power sources, energy storage capacity and number of power loads. The modular power electronics design can accommodate the use of either large Li-Ion cells with individual cell management or, as in the specific SMAP case, small Li-Ion cells without individual cell management.

The SMAP power system architecture is a single string and direct energy transfer system. The power bus voltage is the standard 22V to 36V range.

The power source is a solar array that is approximately 8 square meters of triple junction GaAs cells with a beginning of life power of approximately 1.8kW. The SMAP power bus is controlled by solar array series switching (Figure 2). The solar array segments are switched on or off by the bus controller to provide the power needed by the loads without the use of shunt stages. Three of the solar array segments are sized for "fine" control and six for "coarse" control to reduce the power bus ripple. Further details of the SMAP bus control algorithm are provided in Section 3 of this paper.

The energy storage is a combination of a larger ABSL 8s52p with three smaller 8s10p batteries. The total energy storage capacity is 78 Ah at the beginning of life.

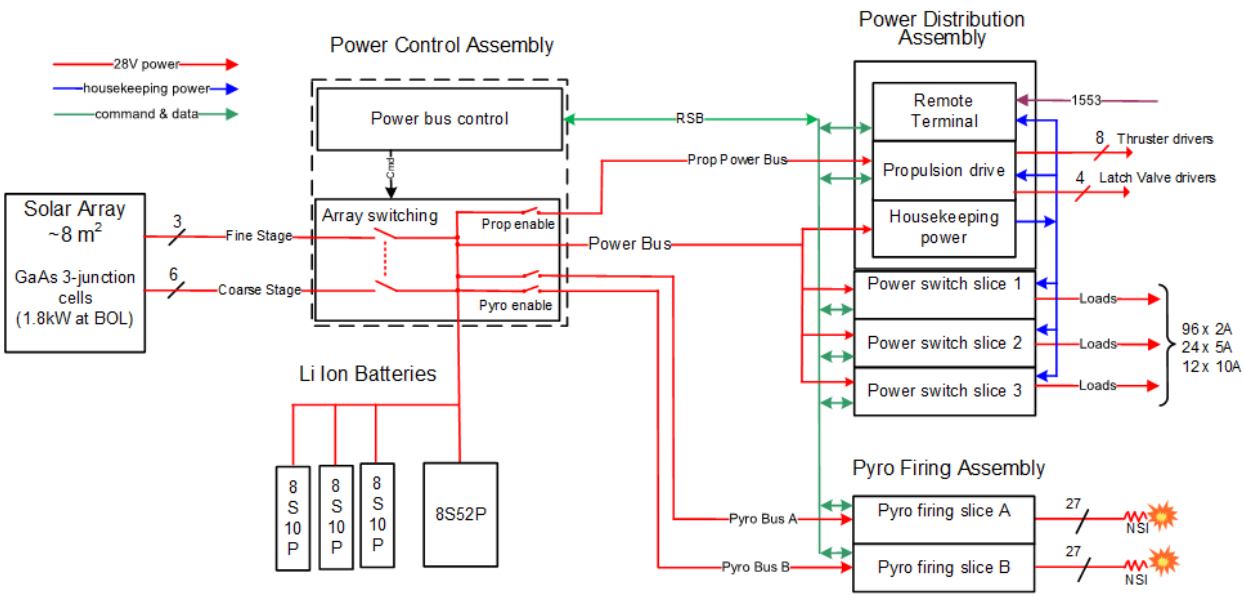

Figure 2: Power System Functional Block Diagram

The SMAP Power Switch Slices (PSSs) distribute power to the spacecraft loads through solid-state switches. The modular architecture of the PSS allows for ease of adding switch cards depending on the number of switches that are needed. Each power switch channel within a PSS switches the "high side" of the power bus to the load in contrast to the historical approach that switches both the "high side" and "return side" of the power bus. SMAP uses a slice packaging configuration that allows for direct heat transfer from the switch card to spacecraft chassis. This improves thermal performance at higher power over the standard wedge-lock 6U VME card format used in previous JPL missions.

The SMAP pyro firing electronics and its associated safety inhibit architecture are fault tolerant. In accordance with NASA Standard Initiator (NSI) specifications, redundant NSIs with redundant pyro switching channels are implemented for each pyro load. The SMAP safety inhibit architecture uses a combination of safe/arm plugs and enable switches as opposed to the embedded arm and enable relays used for previous JPL rover missions. The SMAP inhibit approach saves mass and is more reliable. The pyro firing electronics is packaged in slices that can be added to scale up to meet the requirements of the mission.

3 Power Bus Control Description and Concept Validation

This section provides a description of the SMAP power bus control architecture and the modeling, analysis and validation approaches used.

3.1 Power Bus Control Functional Description

The power bus controller (Figure 3) maintains a target voltage by connecting or disconnecting solar array segments to/from the power bus. If the bus (or battery) voltage is below the target voltage, additional solar array strings are connected to the power bus thus charging the battery until the target voltage is reached. Three solar array circuits, rated at 1A, 2A and 4A, are used for "fine" control and six circuits, rated at 8A each, are used for "coarse" control. If the difference between the battery and target voltages is greater than a few tenths of a volt, the controller charges the battery at a constant rate. As the battery voltage approaches the target voltage, the controller charges the battery at a reduced rate that is in proportion with the error voltage.

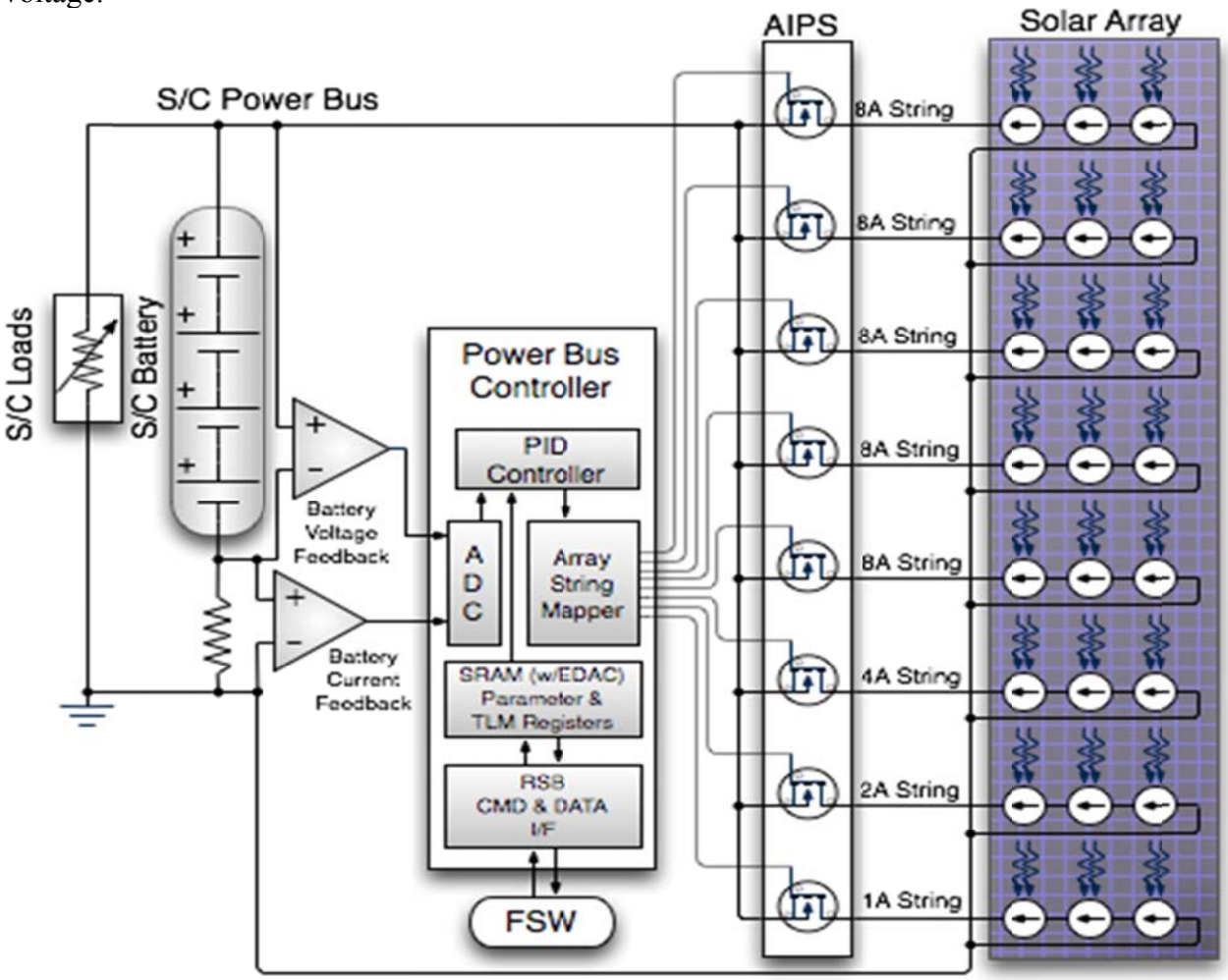

Figure 3: Power Bus Control Functional Diagram

The power bus control is formed of a dual-loop feedback system (Figure 4). An inner loop sets the battery charge current and an outer loop controls the battery voltage. The error voltage from the outer loop defines the battery charge current. The power bus feedback control system uses a PID controller which commands the solar array segment switches. For the SMAP design, the PID derivative coefficient is set to zero and the proportional coefficient is set to a relatively small value. Thus, the integral term dominates the system response.

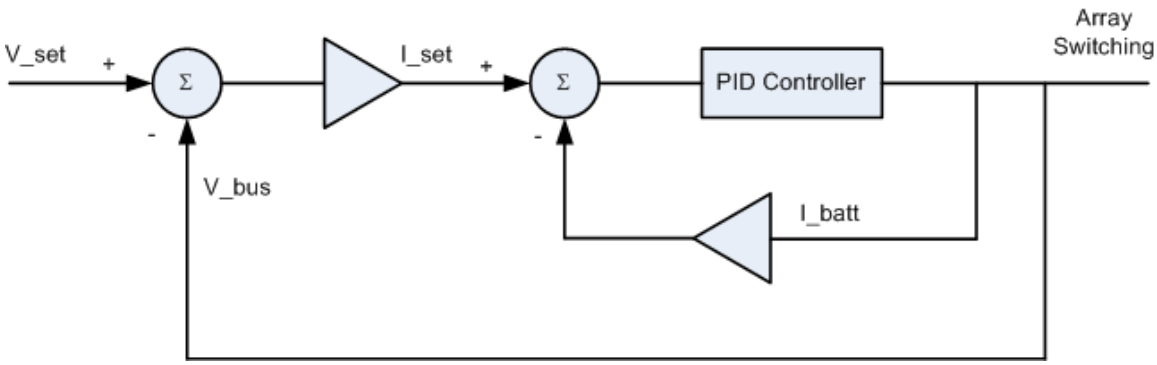

Figure 4: Power Bus Control System

3.2 Power Bus Control Model Behavior

A PSpice behavioral model was developed that simulates the system represented in Figure 4. The validity of the PSpice model was established by comparing the open loop behaviors of the PID Verilog code block in ModelSim to the continuous time analog behavioral model in PSpice (Figure 5). The results of ModelSim and PSpice models were as expected and well correlated. Due to the dominance of the integral term, the PID output response to a 50% duty cycle square wave input is a triangular wave.

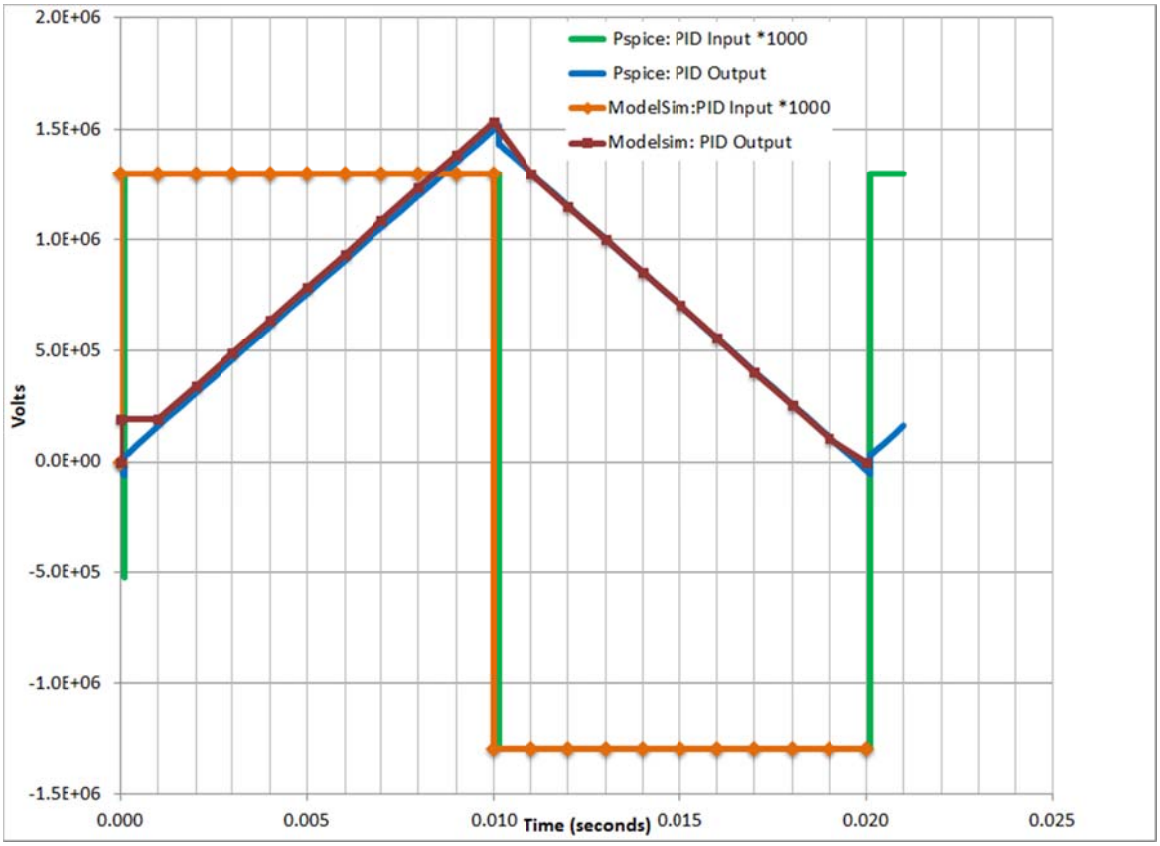

Figure 5: Comparison of ModelSim and PSpice Model PID Responses

3.3 System Transient Response

Modeling the closed loop response to transients shows the large signal response time of the system and can be correlated to the small signal ac stability analysis in the following section. The system response to a 10A load step is shown in Figure 6. During the initial application of the 10A load the battery supplies the additional load current. The solar array segments will then be switched on based on the power demand from the load. As more solar array circuits are switched on, the battery discharge current will decrease and reach zero in approximately 10 milliseconds.

Figure 7 shows the system response to a load decrease of 10A. During the initial removal of the 10A load the excess power from the solar array is used to charge the battery. To compensate for the load decrease solar array circuits will be switched off and the battery charge current will decrease and reach zero in approximately 10 milliseconds.

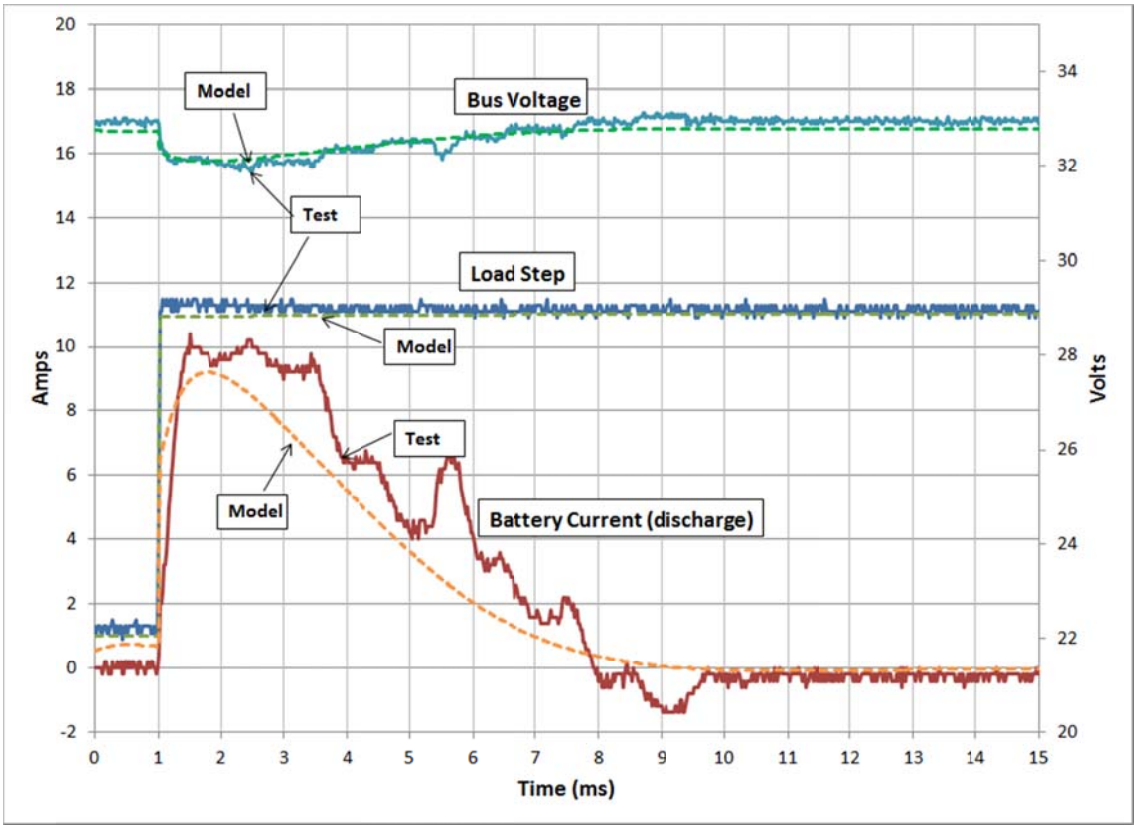

Figure 6: System Transient Behavior during Load Increase

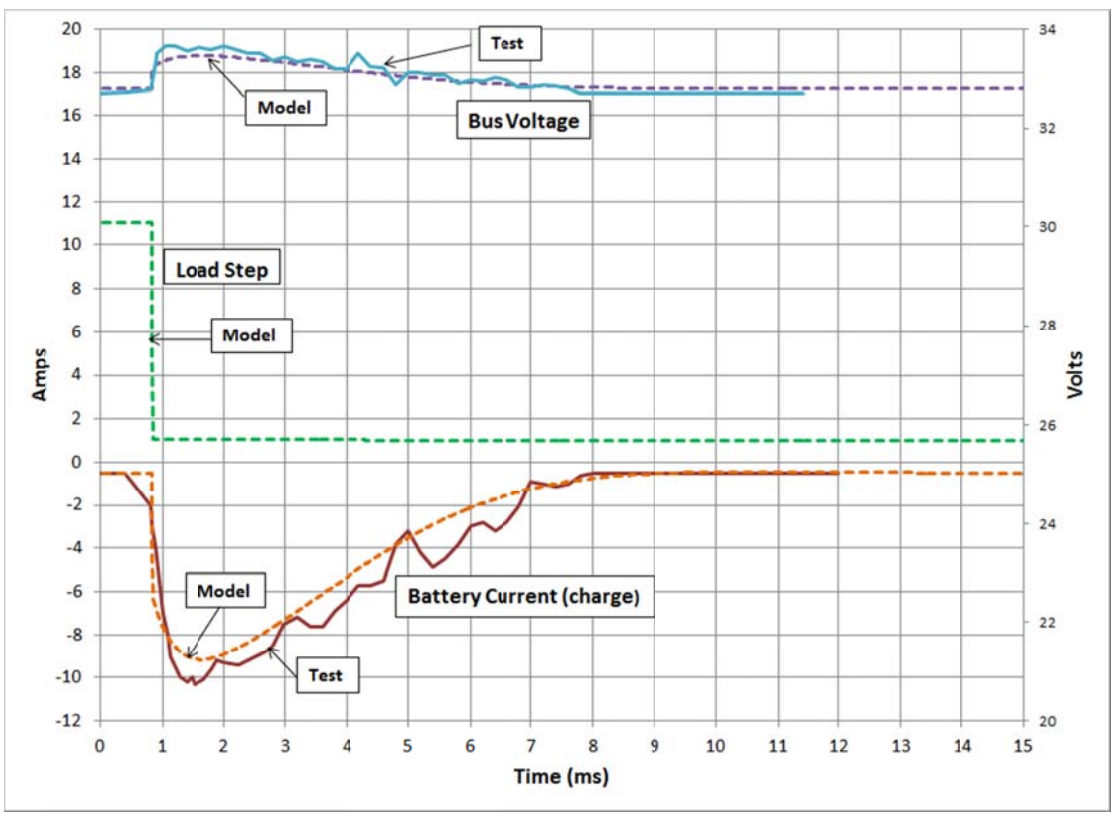

Figure 7: System Transient Behavior during Load Decrease

3.4 System Stability

To assess the stability of the feedback loop system of Figure 4, the open loop gain is measured and represented in Bode diagrams (Figure 8). There is a gain crossover at 51 Hz with a phase margin of 77 degrees. The gain margin is effectively infinite since the phase does not cross the -180 degree line. Thus, the system is robust with adequate stability margins.

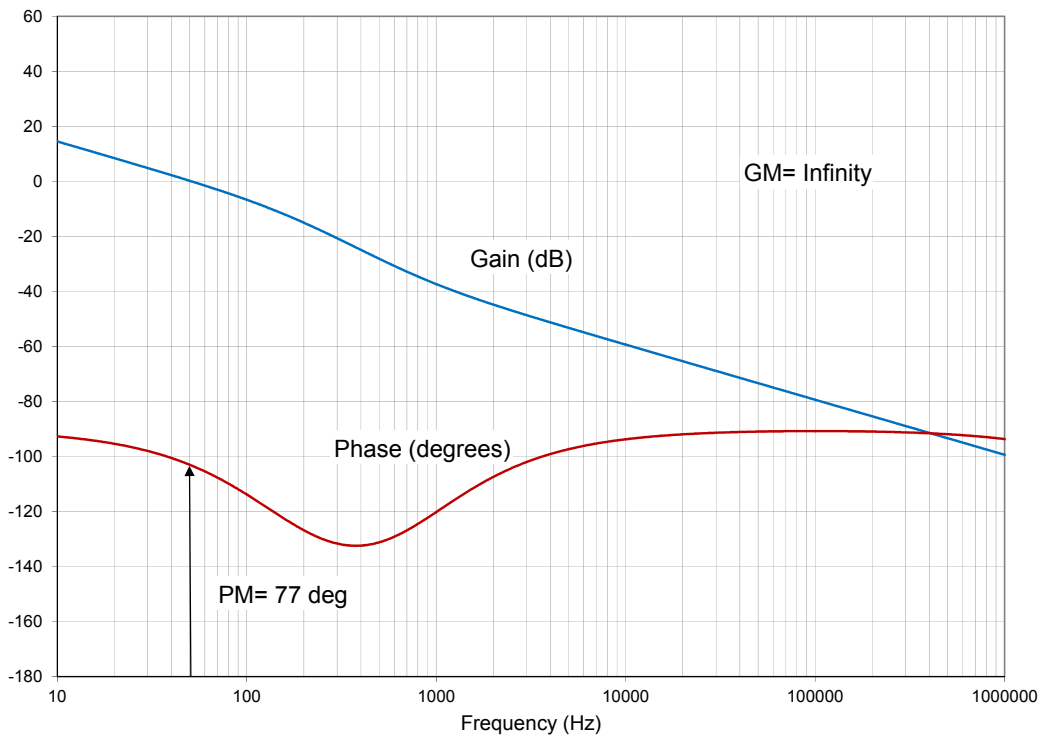

Figure 8: Open-loop Gain of the Power Bus Feedback Control System

4 Conclusions

This paper presents an overview of the SMAP single string power system architecture, which was derived from a fault tolerant modular and scalable architecture at JPL. The modularity of the fault tolerant architecture enabled SMAP to implement a single string version with low development cost. The scalability of the power control, power distribution and pyro firing circuits reduced the amount of electronics that SMAP needed to develop and build. The flexibility of coarse and fine control solar array segment switching allowed SMAP to optimize the number of strings per segment to meet the mission requirements without changing the design.

5 Acknowledgments

The work presented in this paper was carried out at the Jet Propulsion Laboratory, California Institute of Technology, under the sponsorship of the National Aeronautics and Space Administration.

The authors would like to thank Donald Nieraeth, Misrahim Morales, Antonio Ulloa-Severino and Sonny Orellana for their contributions to this work.

6 References

[1] O'Neil, Entekhabi, Njoku and Kellogg, "The NASA Soil Moisture Active Passive (SMAP) Mission: Overview," IEEE Geoscience and Remote Sensing Society (IGARSS) meeting, Honolulu, 2010.

[2] Entekhabi, D., Njoku, E., O'Neill, P. Kellogg K. et al., "The Soil Moisture Active and Passive (SMAP) Mission," Proceedings of the IEEE, Vol. 98, No. 5, May 2010.